International Journal of Engineering

Journal Homepage: www.ije.ir

Bionic Perception Method of Navel Orange Plucking Position Based on Fmincon and PD Angle Control

C. Yu[a,b], K. Liu*[a], L. Lai[b]

[a] *School of Information and Communication, Guilin University of Electronic Technology, Guilin, China*
[b] *School of Information and Communication Engineering, Hezhou University, Hezhou, China*

PAPER INFO

Paper history:
Received 21 July 2022
Received in revised form 11 August 2022
Accepted 21 August 2022

Keywords:
Dynamic Unstructured Environment
Fmincon
Proportional Differential Angle Control
Bionic Perception
Picking Robot

ABSTRACT

In this paper, a bionic perception method of navel orange plucking position based on Fmincon and Proportional Differential (PD) angle control is proposed to solve the problems of wind disturbance and green branches in dynamic unstructured environment. Different from these algorithms that limited to two-dimensional images, this method realizes picking position perception in three-dimensional. Meanwhile, the perception method and the picking robot control algorithm are achieved simultaneously. Firstly, an optimal solution model of the global target rotation angle of the control system based on Fmincon is established to solve the angle optimization problem of robot target approach motion. Secondly, a bionic perception system of plucking position based on PD angle control is constructed to solve specific perception problems. Finally, a joint simulation platform for picking robots based on Solidworks, Adams, and Simulink is given; the validity and accuracy of the algorithm were verified. The experimental results show that the picking accuracy rate is 95%, the angle error of each mechanism and the displacement error are less than 0.5 degrees and 10mm, respectively. The total time from the optimized angle calculation to the system's stability is only about 0.33*s*. This method is suitable for the rapid perception of plucking position and active angle control of picking robots under dynamic unstructured environment.

***doi**: 10.5829/ije.2021.35.11b.22*

1. INTRODUCTION

The rapid developement regarding the automation and artificial intelligence have been strongly pushing the robots to develop technology on agricultural sectors [1-3]. Agricultural robots, as the potential technology to develop intelligent agriculture, take great attention by governments and agricultural sectors [4-6].

The vision system of traditional fruit picking robots are generally based on color space Retinex, Harris and improved Chan-Vese [7-9]. Yu et al. [10] proposed a new strawberry picking robot based on rotating YOLO fruit attitude estimator. Furthermore, for the plucking position of a fruit picking robot, a visual positioning method was proposed by Lei and Lu [11]. Besides, attention model [12], Artificial Neural Network [13,14], Kalman Filter [14],Genetic Algorithm [15], Ant Colony Algorithm [16,17], R-CNN [18], GAN model [19], Greedy Algorithm [20], Synovium Control [21], Deep Learning [22, 23] and Lightweight deep learning methods [24,25] are also used in object perception and control.

However, higher hardware configuration requirements caused by the deep learning are unfriendly to processors with limited performance. Moreover, most algorithms have incomplete detection for low-pixel images under occlusion and different lighting conditions, make it unsuitable for plucking position perception with smaller targets and more precise requirements.

Simultaneously, limited by the computation-intensive, the traditional matching algorithm is not suitable for the plucking position's real-time perception. The shortage of the research on intersection of visual perception and control methods makes it clearly demarcated. The bottleneck problems (for example, the

*Corresponding Author Institutional Email: *liukaidiligent@gmail.com* (Kai liu)

Please cite this article as: C. Yu, K. Liu, L. Lai, Bionic Perception Method of Navel Orange Plucking Position Based on Fmincon and PD Angle Control, ***International Journal of Engineering, Transactions B: Applications***, Vol. 35, No. 11, (2022) 2265-2274

inaccuracy and instability of visual space perception and autonomous picking control of the target) still exist in the low-cost fruit picking robot under the dynamic unstructured environment [26], especially the automatic control and planning in dynamic environments [27].

In this paper, to solve the problems of precise perception of plucking position, a bionic perception method of navel orange plucking position based on Fmincon and PD angle control is proposed. Based on mathematical analysis, combined with the inherent characteristics of crops and rotation angle signal control, the automatic picking operation simulating human picking behavior and the bionic perception method of fruit picking position are established. Meanwhile, a cross-research of the control and perception is also tested in this study. Compared with the perception method based on the target's visual features. This approach can effectively enhance the perception initiative of the picking robot.

The rest of this paper is organized as follows: In section 2, a three-dimensional simulation model and its mathematical model of picking robot are built. In section 3, Fmincon is used to optimize the robot mathematical model's rotation angle. A picking position's bionic perception method based on PD angle control is designed. And in section 4, the experimental results are analyzed. Finally, some concluding remarks are shown in section 5.

2. RELATED WORKS

2. 1. Picking Robot Model Solidworks/Adams 3D Simulation Model. According to the requirements of navel orange fruit picking, a 3D simulation model based on Solidworks/Adams picking arm is designed, as shown in Figure 1.

The model is composed of six parts, which includes the Base, the Rotating Shaft (RS), marked as mechanism 1, the Big Arm (BA), marked as mechanism 2, the Small Arm (SA), marked as mechanism 3, the Wrist Arm (WA) and the Picking Effector (PE). The Wrist Arm and Picking Effector are called End-Effector (EE), marked as mechanism 4, to simplify the analysis. The Picking Effector is composed of Clamped Rod (CR) and two hemispheres of Picking Ball (PB) with a Gap for the mutual bite. The Internal Diameter is represented as IND, while the External Diameter is represented as END.

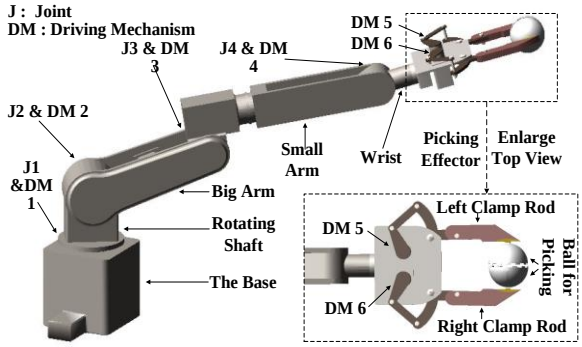

Figure 1. Deposition efficiency on a single square in channel

The corresponding drive is added to each joint (J_i) as the robot's input variable, which is used to control the rotation of each mechanism around the joint in the system model.

The spatial position information of robot's ADAMS model is obtained and provided for the motion solution. Constraints and drivers are added to the imported virtual simulation model to realize the picking robot's kinematics and dynamics simulation.

2. 2. Mathematical Model Developing a "mathematical model" is an important step in robot design and analysis [28]. To further analyze and solve the relative motion and angle relation of each mechanism component, a mathematical analysis model is established based on the three-dimensional simulation $Robot = f\left(x_i, y_i, z_i\right)$, $i = 1,2,3,4$. The target measurement point's initial coordinates are expressed as $m_{ini}\left(x_{ini}, y_{ini}, z_{ini}\right)$, and the target coordinate is $m_{obj}\left(x_{obj}, y_{obj}, z_{obj}\right)$. In this paper's experiment, the spatial coordinate information of the measuring points at the end is output by the three-dimensional simulation software ADAMS.

In order to reduce the complexity and computation, a three-dimensional model is transformed into the two-dimensional mathematical model. There are two different states of the robot as a whole: the thin solid line(—) is used to express the initial state, and the short horizontal line(— • — •) is used to express the target state. Two state curves in *xyz* coordinate are projected onto the *xz* plane to obtain two projected coordinate systems *x'y* and *x''y*. A three-dimensional mathematical model of the picking robot is shown in Figure 2.

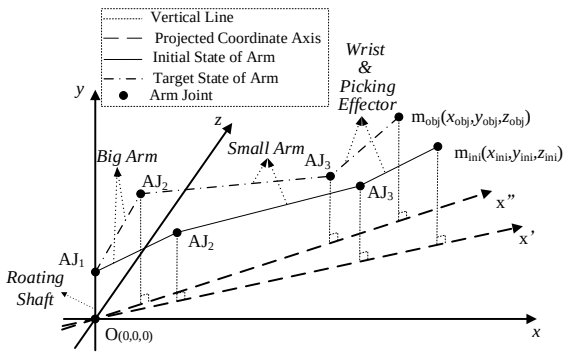

Figure 2. Three Dimensional Mathematical Model of Picking Robot

In the robot's mathematical analysis, the included angle between the two mechanisms is taken as the input variable of the control system. The control system's input is related only to the angle, not to the *xyz* axis coordinates in the original spatial position information. A two-dimensional simplified mathematical model $Robot = g(w_i, y_i)$ is proposed based on the robot's three-dimensional mathematical model and its projection model to simplify the analysis. The simplified model's coordinate axes are *w* and *y*, respectively, where the *w*-axis is the picking robot's projection axis in any state in space, as shown in Figure 3. Where, l_i is the length value of mechanism *i*, $m_{ini}(w_{ini}, y_{ini})$ is the initial coordinate of the end measuring point, $m_{obj}(w_{obj}, y_{obj})$ is the target coordinate, $\theta_{i(i-1)_ini}$ is the initially included angle between mechanism *i* and the connection mechanism, that is, the included angle between each mechanism of the robot in the case of unloaded drive, $\theta_{i(i-1)_obj}$ is the target included angle between mechanism *i* and the connection mechanism. The included angle between the rotating shaft axis and the ground is a constant 90, that is, $\theta_{10_obj}=\theta_{10_ini}=90^{\circ}$.

A mathematical model is built according to Figure 1 to solve the picking robot's end-effector's operation control problem, as shown in Figure 4. The coordinate information of the left and right endpoints is used as the control system's input state variable. L_{CR} is assumed as the length of the left and right clamp rods of the end-effector, and the left and right clamp rods are driven by Drive five and Drive six to carry out picking movement, respectively. L_{DM} and l_{CR} are assumed as the distance between Drive five and Drive six and the clamp rod's length projected on the line of endpoints, respectively. Furthermore, θ_{PA} is assumed as the included angle between the clamp rod and its perpendicular. θ_{PA} is assumed as the input of the real-time state variable of the control system, which initial included value is 1.11472°. It is varied when the picking task is operating.

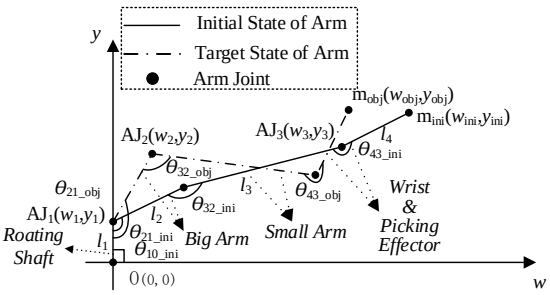

Figure 3. A Two-Dimensional Simplified Mathematical Model of a Picking Robot

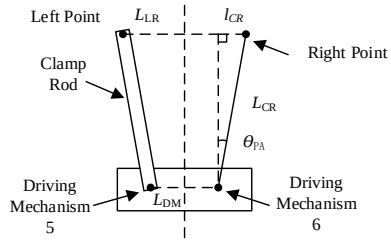

Figure 4. Two Dimensional Mathematical Model of Robot End-Effector

Equation (1) shows the included angle θ_{PA} between the robot end-effector's clamp rod and its perpendicular.

$$\theta_{PA} = arcsin\frac{l_{CR}}{L_{CR}} \tag{1}$$

The length value projected by the clamp rod on the endpoint line is shown in Equation (2).

$$l_{CR} = (L_{LR} - L_{DM})/2 \tag{2}$$

where, L_{LR} is the distance between the left and right endpoints $L(x_L, y_L, z_L)$ and $R(x_R, y_R, z_R)$ of the clamp rod, as shown in Equation (3).

$$\begin{cases} L_{LR} = \left(\sum_{h=x}^{z}(h_L - h_R)^2\right)^{1/2} \\ h = (x, y, z) \end{cases} \tag{3}$$

3. PROPOSED METHOD

3. 1. The Optimal Solution Method of Robot Mechanism's Rotation Angle Based on Fmincon Method

In this section, the nonlinear optimization equation of the robot's angle control is established according to the picking robot's established mathematical model. The robot's nonlinear equation inclued absolute values, sines and coines, inequalities, and equality constraints. A global optimal rotation angle $\Delta\theta_{i(i-1)}$ solution method based on Fmincon is designed to solve nonlinear constrained equations. The Fmincon is provided by the MATLAB optimization system toolbox.

$\Delta\theta_{i(i-1)}$ is assumed as the difference between the initial included angle $\theta_{i(i-1)_ini}$ and the target included angle $\theta_{i(i-1)_obj}$ of each mechanism, which can be solved by Equation (4).

$$\begin{cases} \Delta\theta_{i(i-1)} = \theta_{i(i-1)_obj} - \theta_{i(i-1)_ini} \\ i = 1,2,3,4 \end{cases} \tag{4}$$

Set $\rho_{ij}(l_i, \theta_{ij_obj})$ and θ_{ij_obj} as the polar coordinates of mechanism *i* relative to mechanism *j* and the included

angle between mechanism i and mechanism j, where j=0,1,2,3 and $j<i$, and mechanism j=0 represents the w-axis of the ground, in other words, θ_{i0_obj} represents the polar coordinate included angle of mechanism i relative to ground w-axis, formulated as Equation (5).

The optimization equation of rotation angle $\Delta\theta_{i(i-1)}$ of the robot mechanism based on the mathematical model is designed, formulated as Equation (6).

$$\begin{cases} \theta_{ij_obj} = \left(\theta_{i(i-1)_ini} + \Delta\theta_{i(i-1)}\right) - \sum_{k=j}^{i-j-1}\left(180^\circ - \left(\theta_{(k+1)k_ini} + \Delta\theta_{(k+1)k}\right)\right) \\ 0 \le j \le i-2 \end{cases} \tag{5}$$

$$\begin{aligned} & min \quad |\Delta\theta_{21}| + |\Delta\theta_{32}| + |\Delta\theta_{43}| \\ & s.t. \begin{cases} \sum_{i=1}^{4}\left(\theta_{i(i-1)_ini} + \Delta\theta_{i(i-1)}\right) + \theta_{end} + 90^\circ = (6-2)*180^\circ \\ \sum_{i=1}^{4} l_i \, sin\left(\theta_{i0_obj}\right) = y_{obj} \\ \sum_{i=1}^{4} l_i \, cos\left(\theta_{i0_obj}\right) = w_{obj} \\ \Delta\theta_{10} = 0^\circ \\ 45^\circ \le \theta_{end} \le 90^\circ \\ max\left\{-120^\circ, -\left(\theta_{i(i-1)_ini} + \Delta\theta_{i(i-1)}\right)\right\} \le \Delta\theta_{i(i-1)} \le min\left\{120^\circ, 360^\circ - \left(\theta_{i(i-1)_ini} + \Delta\theta_{i(i-1)}\right)\right\} \\ i = 1,2,3,4 \end{cases} \end{aligned} \tag{6}$$

The intention of objective function is to ensure each drive's minimum power consumption, namely the minimum sum of rotation angles. The constraint function is determined in polar coordinates to solve the projection distance between the w-axis and y-axis. The included angle θ_{end} between the end-effector and the y-axis is designed to ensure that the end-effector position conforms to the bionics and picking requirements during the picking.

Three parts are included in the optimization equation's constraint conditions: the global angle constraint, the coordinate axis projection distance constraint, and the permissible range constraint of the rotation angle of each mechanism. Among them, the purpose of the angle constraint in the global range and the distance projected by the coordinate axis is to ensure that the robot picking actuator accurately reaches the target position. In contrast, the range of rotation angle variation is designed to prevent the collision of various mechanisms in the process of moving. According to the robot's movement characteristics, the maximum bidirectional reference angle of rotation of the joint mechanism is taken to be 120 degrees to prevent the system from being out of balance due to too large angle change. The rotation angle is positive counterclockwise.

$\Delta\theta_{Roating_x}$ is assumed as the rotating shaft's rotation angle concerning the x-axis in the three-dimensional model $Robot = f\left(x_i, y_i, z_i\right)$, formulated as Equation (7), where the target coordinate of the end measurement point is named as $m_{obj}\left(x_{obj}, y_{obj}, z_{obj}\right)$.

$$\Delta\theta_{Roating_x} = arctan\frac{z_{obj}}{x_{obj}} - arctan\frac{z_{ini}}{x_{ini}} \tag{7}$$

With the nonlinear optimal angle objective Equation (5) to (7), the ideal rotation angle $\Delta\theta_{i(i-1)}$ is output to the Simulink control system, and the running time t is recorded.

3. 2. Bionic Perception Method Based on PD Angle Control In this section, a real-time feedback control system of PD based on MATLAB/Simulink is designed to control a picking robot's picking operation in a dynamic unstructured environment. The two parts of the system form a closed loop based on Simulink and Adams, in which the 3D module outputs the displacement and included angle values of each mechanism and measurement points as the variable input of the control module. The rotation angle modulated by each picking robot mechanism is used as the output of PD angle control system. The closed-loop control method of picking system of picking robot is shown in Figure 5. The rotation angle $\Delta\theta_{i(i-1)}$ of the robot mechanism is used as the control system's initial input and continues the whole control process. The control algorithm of the intelligent picking system based on PD angle control is shown in ALGORITHM 1. where k is the sequence number of complete closed-loop output formed by the control system.

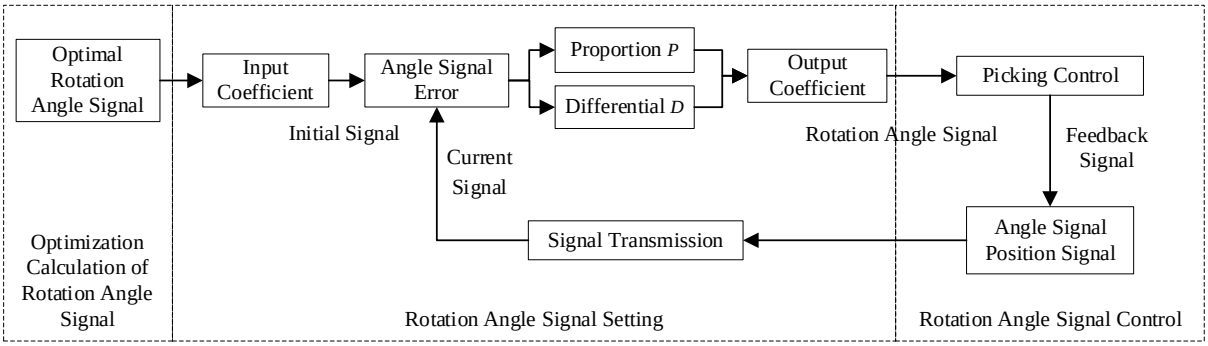

Figure 5. Deposition efficiency on a single square in channel

ALGORITHM 1. PD Control of Angle

1: Algorithm Start

2: Calculate the rotation angle value $\Delta\theta_{i(i-1)}$ of each mechanism.

3: The input coefficient $K_{in}=\frac{1}{0.2857}$ is introduced, the rotation angle is going to be $\Delta\theta_{i(i-1)}{}' = K_{in}\times\Delta\theta_{i(i-1)}$;

4: Calculate the difference $e(k)$ between $\Delta\theta_{i(i-1)}{}'$ and the rotation angle $\Delta\theta_{i(i-1)now}$ in the current state of the system, $e(k)=\Delta\theta_{i(i-1)}{}'-\Delta\theta_{i(i-1)now}$;

5: Calculate the rate of change of per unit sampling time $ec(k)=\frac{de}{dt}$;

6: PD Parameters: The empirical method is used to set the coefficient of proportion $K_p=2$ and differential $K_d=-0.01$;

7: PD Output : $u(k)=K_p e(k)+K_d ec(k)$;

8: The output coefficient K_{out}=0.2 is introduced, the rotation angle is going to be $\Delta\theta_{i(i-1)}{}''=K_{out}\times u(k)$;

9: Enter $\Delta\theta_{i(i-1)}{}''$ into the robot model, and get the current position $m_{now}(x_{now},y_{now},z_{now})$ and the current angle $\theta_{i(i-1)now}$.

10: According to $m_{now}(x_{now},y_{now},z_{now})$ and current angle $\theta_{i(i-1)now}$ of each mechanism, the rotation angle $\Delta\theta_{i(i-1)now}=\theta_{i(i-1)now}-\theta_{i(i-1)_ini}$ is calculated.

11: Clamping Rod Operation: When time t=0.1s, the end-effector's clamp rods rotation makes the picking ball close, where, the rotation angle is θ_{PA}=9.2° .

12: Bionic Perception: When time t=0.15s, the rotation angle $\Delta\theta'_{43}=\Delta\theta_{43}-5$ of the system's end-effector will automatically change, that is, rotate clockwise 5° to realize the bionic perception operation.

13: Feedback Control: Go back to Step 4 and calculate the angle error e and angle value until stable;

14: Algorithm End

The control system in a dynamic unstructured environment eliminates the robot mechanism rotation angle's motion error to ensure the accuracy and robustness in picking control. In this paper, an optimized PD angle control method is proposed based on the input and output auxiliary coefficients K_{in} and K_{out} . Set K_p and K_d as the proportional and differential coefficients of the PD angle control system, respectively. Wherein, the coefficient K_p and K_d of proportion and differentiation in the PD angle control method are determined by the empirical method. In the picking experiment of the picking robot, the picking control system is in the most stable state when K_p and K_d take the above values, which is the basis for the fruit picking experiment's successful realisation. Moreover, set $m_{now}(x_{now},y_{now},z_{now})$, $\theta_{i(i-1)now}$ and $\Delta\theta_{i(i-1)now}$ as the current coordinate of the end measuring point, the included angle, and each mechanism's rotation angle under the current system state, respectively. $\Delta\theta_{i(i-1)now}$, as shown in Equation (8).

$$\Delta\theta_{i(i-1)now}=\theta_{i(i-1)now}-\theta_{i(i-1)_ini} \tag{8}$$

3. 3. Bion Bionic Perception Method of Plucking Position Based on Control Precise perception of the plucking position is essential for the success or failure of fruit picking without damage. The current algorithm has a relatively mature visual perception of navel orange and other fruits. However, few spatial perception methods for fruit plucking position in the dynamic unstructured environment, and these methods are less effective.

A bionic perception method of plucking position based on PD angle control to solve the above problems. The left and right clamp rods of the end-effector are opened, and the navel orange is included in the picking ball when the robot end-effector reaches the navel orange. Moreover, the navel orange leaves and branches

can protrude through the gaps between the picking balls. And then, the end-effector rotates clockwise for θ_w with the navel orange. Normal-growths navel oranges will cling to the picking ball's inner surface due to the bionics and plant branches' inherent properties. Moreover, we set the contact point as the picking point, as shown in Figure 6.

Navel oranges, for example, the Fuchuan navel orange we collected at the agricultural base of Guangxi Zhengfeng Group, are about 70-85*mm* in diameter, 250-300*g* in mass, and 3-5*mm* in diameter of terminal branches. Based on the design principles of the navel orange plant's tensile strength and the quality range of navel orange fruit, the rotation angle $\theta_w = -5^\circ$ is designed to prevent excessive angle or operation amplitude. Set d_w as the displacement of navel orange in the end-effector, formulated as Equation (9). The elastic modulus, bending strength, breaking modulus and ultimate stress of navel orange branches are 8.5 *GPa*, 193.2 *MPa*, 67.3 *MPa* and 45.3 *MPa*, respectively.

$$d_w = 2 \times l_4 \times sin\left(\frac{|\theta_w|}{2}\right) \tag{9}$$

According to Equation (9), the displacement d_w at the end measuring point is 6.2*mm*, which conforms to the picking process's bionics practice.

Compared with the perception method based on visual features, our method has more robust initiative, which can reduce the multiple losses of time and economy caused by the inaccurate perception of plucking position.

4. EXPERIMENTS AND RESULTS

4. 1. Experimental Platform The experimental platform is a 64-bit Windows 10 system equipped with Intel Core I7-6700 processor. MATLAB 2018B and Adams 2018 are used to construct the simulation system, and Solidworks 2012 is used to build the corresponding 3D model. A joint simulations is created with MATLAB/ Simulink and Adams Control, Communication Interval of MATLAB/Simulink control system is set to 5*ms*.

4. 2. Results In this section, the end-effector (marked as mechanism 4) of picking robot is taken as a concrete object for quantitative analysis to verify the proposed perception and control algorithm. We randomly select the target coordinates (377.862, 703.386, -1541.232), and the target rotation angle $\Delta\theta_{43}$ based on Fmincon method is 13.87760°. And the angle change and response speed for the algorithm are tracked. The analysis diagram of rotation angle $\Delta\theta_{43now}$, current angle θ_{43now}, the coordinate of the end measuring point and the angle error *e* of the end-effector are shown in Figures 7, 8, 9 and 10, respectively.

Figures 7 and 8 show that the angle control system based on the algorithm can achieve system stability within 0.06*s* during the prophase perception and the bionic perception. The end measuring point on the end-effector reaches the target position quickly at the same time. The analysis of Figure 9 shows that the end-effector finally tends to set the target point and remains stable. At the beginning of the bionic perception operation, the end-effector change's angle and coordinates correspondingly, but there is only a small disturbance for the overall operation, which has little influence. According to the analysis of Figure 10, the difference in angle and displacement between the initial state of the robot and the target state is large, resulting in a large error from the initial state to the first working moment of the system. The error's variation value is relatively drastic, but eventually, all tend to zero and maintain a stable state.

A global analysis result for the robot is presented here. When the system randomly selects any coordinate

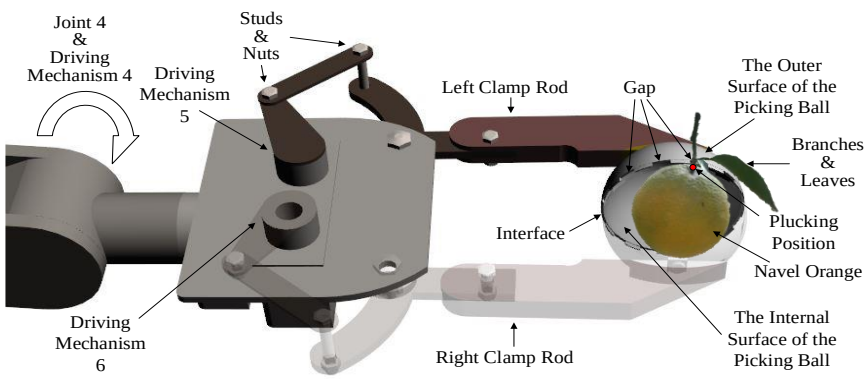

Figure 6. Bionic Perception Diagram of Plucking Position Based on System Control

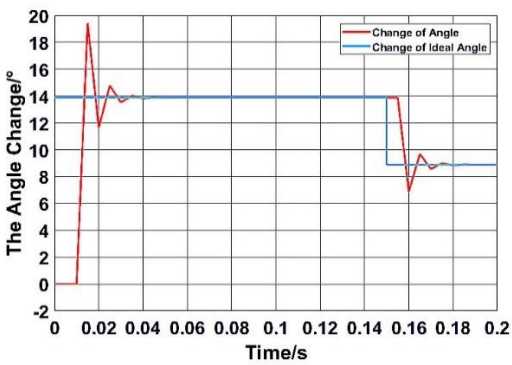

Figure 7. Rotation Angle $\Delta\theta_{43now}$ Tracking Diagram of End-Effector

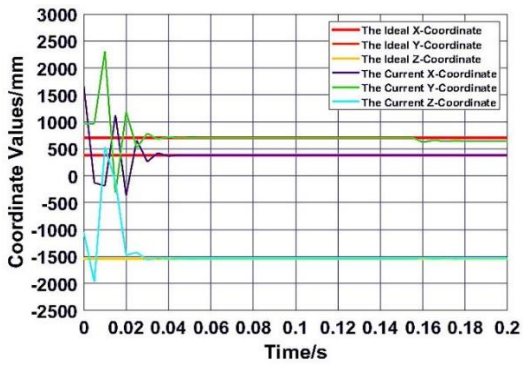

Figure 9. Coordinate Displacement Tracking Diagram of End Measuring Point

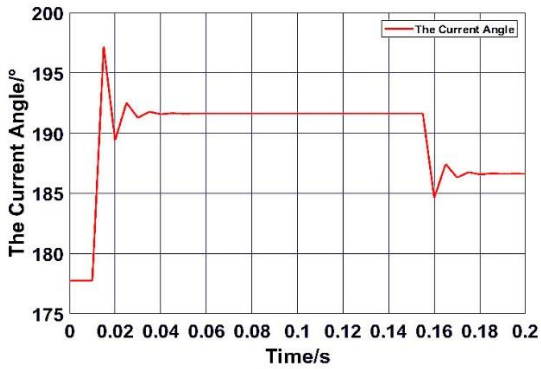

Figure 8. Current Angle θ_{43now} Tracking Diagram of End-Effector

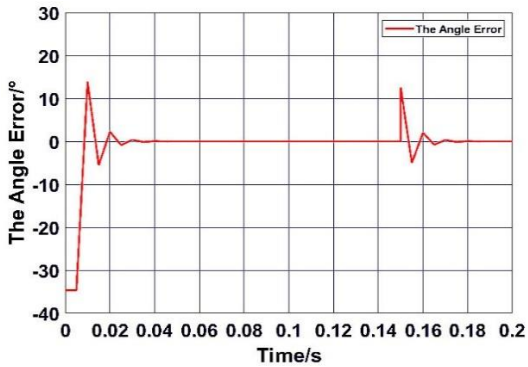

Figure 10. Analysis Diagram of Rotation Angle Error *e* of End-Effector

point, the average consumption time of calculating the rotation angle based on Fmincon method is 0.21021*s*. And when the system is stabilization, the rotation angle error *e* and its standard deviation SD of each mechanism are shown in Table 1. Where, PP and BP represent End-Effector in the prophase perception stage and the bionic perception stage, respectively.

As shown in Table 1, each mechanism of the picking robot's rotation angle error is 10^{-3} level. Since the picking robot base bears most of the mass of the mechanism, the rotation angle error of the shaft is large, which is about 0.2°. And the standard deviation of each picking robot mechanism's rotation angle is generally 0.0004-0.0013, and the maximum standard deviation appears at the

TABLE 1. Rotation angle error of picking robot

No.	Error *e*/°					SD				
	RS	BA	SA	End-Effector		RS	BA	SA	EE	
				PP	BP				PP	BP
1	-0.21754	0.00220	-0.00330	0.00000	-0.00025	0.0932204	0.0007121	0.0013467	0.0006198	0.0004836
2	-0.21220	0.00310	-0.00470	0.00070	0.00040					
3	-0.16180	0.00080	-0.00150	0.00000	-0.00025					
4	-0.12807	0.00110	-0.00310	0.00120	0.00090					
5	-0.15860	0.00170	-0.00340	0.00100	0.00060					
Average	0.17579	0.00144	0.00238	0.00077	0.00069			-		

rotation axis RS and does not exceed 0.1. And the displacement error *ed* of the end measuring point and its standard deviation SD is shown in Table 2.

As shown in Table 2, the absolute value of displacement error *ed* of each mechanism relative to the target point of the picking robot is within the range of 0.1*mm*-5*mm*, and the mean displacement error values in *x*, *y* and *z*-axis directions are 1.52819*mm*, 4.50943*mm* and 3.15513*mm* respectively. Moreover, the standard deviations are 1.2165539, 0.681218 and 1.6084507, respectively. The mean displacement error of the straight-line distance between the measuring point at the end of the end-effector and the target point is 6.00608*mm*, and the standard deviation is 1.0408286. The system still has good accuracy in controlling the whole robot.

The accuracy evaluation index of robot picking is proposed to verify the performance of PD angle control and bionic perception method in dynamic unstructured environment: Set d_e as the spatial distance between the coordinates $m_{now}\left(x_{now}, y_{now}, z_{now}\right)$ of the end measuring point end-effector and the target coordinates $m_{obj}\left(x_{obj}, y_{obj}, z_{obj}\right)$ in the prophase perception. And $d_{e\,max}$ is the maximum error. It is the successful picking when d_e is less than the maximum error $d_{e\,max}$. We designed $d_{e\,max}$ to be 10 *mm* because of the dynamic unstructured environment's interference and the biophysical and inclusive nature of the picking ball.

T_X is the number of experiments when d_e is less than $d_{e\,max}$;while T_D is the number of experiments when d_e is greater than $d_{e\,max}$. In this paper, the picking perception accuracy (*P*) of the robot under different rotation angles is calculated, as shown in Equation (10).

$$P = \frac{T_X}{T_X + T_D} \times 100\% \tag{10}$$

The algorithm proposed in this paper has been tested many times under the condition of setting coordinates at will. According to Equation (9), the picking perception accuracy rate is 95%, which has a good picking effect. Comparison tests are conducted on the algorithms, and the results of different algorithms are shown in Table 3. Given the impact of the implementation methods and evaluation indexes of different algorithms on the experiment, this paper adopts the final picking accuracy *P* as the basic principle of comparison. Other methods compared to the Zhuang's method, the percentage of picking accuracy improved is marked by γ, and the percentage of time reduced is marked by λ other method's.

It can be seen from Table 3 that the plucking position perception method of the picking robot in this paper has better picking accuracy and faster perception time compared with other methods with similar functions. Different from these algorithms that limited to two-dimensional images, this method realizes picking

TABLE 2. Displacement error of picking robot

No.	Error *ed*/mm				SD			
	x	y	z	Sum	x	y	z	Sum
1	1.66000	4.30000	4.10700	6.17358				
2	0.83300	3.94700	2.63800	4.81993				
3	0.70010	4.93020	3.64820	6.17304	1.2165539	0.681218	1.6084507	1.0408286
4	-0.46900	4.80480	2.48600	5.43013				
5	0.09200	4.63700	2.97900	5.51223				
Average	1.52819	4.50943	3.15513	6.00608		-		

TABLE 3. Picking perception accuracy under different methods

Algorithm	Method	Picking Point Dimension	*P*/%	γ/%	Time/*s*	λ/%
Zhuang et al. [8]	Computer Vision-based Localisation	2D Image	83.0	-	1.06	-
Xiong et al. [7]	Morphological+Min-Circumscribed Rectangle+ Hough	2D Image	86.3	3.98	0.46	37.5
Lei et al. [11]	Color Modol+Corner Detection+K-means	2D Image	89.2	7.47	0.65	38.68
Yu et al. [10]	R-YOLO	2D Image	84.35	1.63	0.056	94.71
Algorithm in this paper	Fmincon+PD Angle Control	3D Dimensions	95.0	14.46	0.33	68.88

position perception in three-dimensional. Meanwhile, the perception method and the picking robot control algorithm are achieved simultaneously. In addition, the bionic perception algorithm based on PD angle control in this paper realizes the plucking position perception and the picking behavior at the same time, which further saves time for the operation of the picking robot.

5. CONCLUSION

In this paper, a bionic perception method based on Fmincon and PD angle control is proposed to solve the problem of poor perception accuracy of navel orange and its plucking position in the agricultural dynamic unstructured environment.

Firstly, Fmincon method is used to optimize the value of target rotation angle based on three-dimensional simulation model in dynamic unstructured environment. Then, the picking control based on the optimized PD algorithm is carried out according to the target rotation angle. Finally, a bionic perception method based on system control is designed for the spatial perception of plucking position, and the validity and accuracy of the algorithm are verified by experiments.

The experimental results show that the picking accuracy of the bionic perception algorithm based on Fmincon method and optimized PD angle control is 95% and the time is 0.33*s*, which can effectively solve the environmental interference of low-cost picking robot in a dynamic unstructured environment and the problem of low navel orange perception accuracy. Different from other algorithms, perception method and picking robot control are achieved simultaneously. The method is simple, does not need expensive equipment, and is easier to use in developing countries and regions.

However, compared with the faster processing speed, this paper's real-time processing needs to be further improved. Higher real-time performance and its testing in the entity will focus on this paper in the future. With the increasing concern of food security and the rapid development of artificial intelligence, it is hoped that the research in this paper can contribute to the development of fast, efficient, accurate and low-cost picking robots.

6. ACKNOWLEDGMENT

This work is financially supported by the Dean Project of Guangxi Key Laboratory of Wireless Wideband Communication and Signal Processing (20171016), the Key Cultivation Project of Hezhou University (2019ZDPY02), the Natural Science Funding Project of Hezhou University (2019ZZZK01), the National Natural Science Foundation of China (6154055, 61863011), and the Science Research and Technology Development Program of Hezhou (No. 1707041).

7. REFERENCES

1. Klerkx, L., Jakku, E., and Labarthe, P. “A review of social science on digital agriculture, smart farming and agriculture 4.0: New contributions and a future research agenda”, ***NJAS-Wageningen Journal of Life Sciences***, Vol. 2019, No. 90, (2019), 100315. doi: 10.1016/j.njas.2019.100315.
2. Vasconez, J. P., Kantor, G. A., and Cheein, F. A., A. “Human–robot interaction in agriculture: A survey and current challenges.” ***Biosystems Engineering***, Vol. 2019, No. 179, (2019), 35-48. doi: 10.1016/j.biosystemseng.2018.12.005.
3. Fountas, S., Espejo-García, B., Kasimati, A., Mylonas, N., and Darra N. “The Future of Digital Agriculture: Technologies and Opportunities.” ***IT Professional***, Vol. 22, No. 1, (2020), 24-28. doi: 10.1109/MITP.2019.2963412.
4. Bhimanpallewar, R. N., and Narasingarao, M. R. “AgriRobot: implementation and evaluation of an automatic robot for seeding and fertiliser microdosing in precision agriculture.” ***International Journal of Agricultural Resources, Governance and Ecology***, Vol. 16, No. 1, (2020), 33-50.
5. Moundekar, D., Nakhate, P., Ghosh, S., and Kasetwar, A. R. “Agricultural Robot (Agribot): A Future of Agriculture.” ***Agriculture International***, Vol. 6, No. 04, (2020), 06-10.
6. Leitner, J. “Picking the right robotics challenge.” ***Nature Machine Intelligence***, Vol. 1, No. 3, (2019), 162-162. doi: 10.1038/s42256-019-0031-6.
7. Xiong J., Liu, Z., Lin, R., Bu, R., He, Z., Yang, Z., and Liang, C. “Green Grape Detection and Picking-Point Calculation in a Night-Time Natural Environment Using a Charge-Coupled Device (CCD) Vision Sensor with Artificial Illumination.” ***Sensors***, Vol. 18, No. 4, (2018), 969-985. doi:10.3390/s18030969.
8. Zhuang, J., Hou, C., Tang, Y., He, Y., Guo, Q., Zhong, Z., and Luo, S. “Computer vision-based localisation of picking points for automatic litchi harvesting applications towards natural scenarios.” ***Biosystems Engineering***, Vol. 187, (2019), 1-20. doi: 10.1016/j.biosystemseng.2019.08.016.
9. Ma, Y., Zhang, W., and Qureshi, W. S. “Autonomous Navigation for a Wolfberry picking robot Using Visual Cues and Fuzzy control.” ***Information Processing in Agriculture***, (2020), doi: 10.1016/j.inpa.2020.04.005.
10. Yu, Y., Zhang, K., Liu, H., Yang, L., and Zhang, D. “Real-Time Visual Localization of the Picking Points for a Ridge-Planting Strawberry Harvesting Robot.” ***IEEE Access***, Vol. 2020, No. 8, (2020), 116556-116568. doi: 10.1109/ACCESS.2020.3003034.
11. Lei, W., and Lu, J. “Visual positioning method for picking point of grape picking robot (in Chinese).” ***Jiangsu Journal of Agricultural Sciences***, Vol. 36, No. 4, (2020), 1015-1021. doi: 10.3969/j. issn.1000-4440.2020.04.029.
12. Wu, B., Akinola, I., Gupta, A., Xu, F., Varley, J., Watkins-Valls, D., and Allen, P. K. “Generative Attention Learning: a GenerAL framework for high-performance multi-fingered grasping in clutter.” ***Autonomous Robots***, Vol. 2020, No. 44, (2020), 971-990. doi: 10.1007/s10514-020-09907-y.
13. Esfandian, N., and Hosseinpour, K. "A clustering-based approach for features extraction in spectro-temporal domain using artificial neural network." ***International Journal of Engineering, Transactions B: Applications***, Vol. 34, No. 2, (2021), 452-457. doi: 10.5829/IJE.2021.34.02B.17

14. Siddharth, D., Saini, D. K. J., and Singh, P. "An Efficient Approach for Edge Detection Technique Using Kalman Filter with Artificial Neural Network." ***International Journal of Engineering, Transactions C: Aspects***, Vol. 34, No. 12, (2021), 2604-2610. doi: 10.5829/ije.2021.34.12c.04

15. Lin, C. Y., Gussu, T. W., and Tsai, Y. N. "A multi objective genetic algorithm approach to a design parameter generation for a robot platform on three omnidirectional wheels." ***Journal of the Chinese Institute of Engineers***, Vol. 40, No. 8, (2017), 659-668. doi: 10.1080/02533839.2017.1384327.

16. Wong, C. C., Feng, H. M., Lai, Y. C., and Yu, C. J. "Ant Colony Optimization and image model-based robot manipulator system for pick-and-place tasks." ***Journal of Intelligent & Fuzzy Systems***, Vol. 36, No. 2, (2019), 1083-1098. doi: 10.3233/JIFS-169883.

17. Karami, M., Tavakolpour-Saleh, A. R., and Norouzi, A. "Optimal Nonlinear PID Control of a Micro-Robot Equipped with Vibratory Actuator Using Ant Colony Algorithm: Simulation and Experiment." ***Journal of Intelligent & Robotic Systems***, Vol. 2020, No. 99, (2020), 1-24. doi: 10.1007/s10846-020-01165-5.

18. Yu, Y., Zhang, K., Yang, L., and Zhang, D. "Fruit detection for strawberry harvesting robot in non-structural environment based on Mask-RCNN." ***Computers and Electronics in Agriculture***, Vol. 2019, No. 163, (2019), 104846. doi: 10.1016/j.compag.2019.06.001.

19. Shahbakhsh, Mostafa Balouchzehi, and Hamid Hassanpour. "Empowering Face Recognition Methods Using a GAN-based Single Image Super-Resolution Network." ***International Journal of Engineering, Transactions A: Basics***, Vol. 35, No. 10, (2022). doi: 10.5829/ije.2022.35.10a.05

20. Wang, W., and Fu B. "Target Recognition Method of Eggplant's Picking Robot under Natural Environment." ***Journal of Anhui Agricultural Sciences***, Vol. 2019, No. 18, (2019), 64.

21. Chen, W., Xu, T., Liu, J., Wang, M., and Zhao, D. "Picking robot visual servo control based on modified fuzzy neural network sliding mode algorithms." ***Electronics***, Vol. 8, No. 6, (2019), 605. doi: 10.3390/electronics8060605.

22. Liu, W., Anguelov, D., Erhan, D., Szegedy, C., Reed, S., Fu, C., Y., and Berg, A., C. "SSD: Single shot multibox detector." European Conference on Computer Vision, Cham, September, (2016), 21-37. doi: 10.1007/978-3-319-46448-0_2.

23. Jin, Z., Sun, W., Zhang, J., Shen, C., Zhang, H., and Han, S. "Intelligent Tomato Picking Robot System Based on Multimodal Depth Feature Analysis Method." ***E&ES***, Vol. 440, No. 4, (2020), 042074. doi: 10.1088/1755-1315/440/4/042074.

24. Howard, A. G., Zhu, M., Chen, B., Kalenichenko, D., Wang, W., Weyand, T., and Adam, H. "MobileNets: Efficient convolutional neural networks for mobile vision applications." arXiv preprint, (2017), 1704.04861.

25. Zhang, X., Zhou, X., Lin, M., and Sun, J. "Shufflenet: An extremely efficient convolutional neural network for mobile devices." Proceedings of the IEEE Conference on Computer Vision and Pattern Recognition, (2018), 6848-6856.

26. Bloch, V., Bechar, A., and Degani, A. "Development of an environment characterization methodology for optimal design of an agricultural robot Industrial Robot." ***An International Journal***, Vol. 44, No. 1, (2017), 94-103. doi: 10.1108/IR-03-2016-0113.

27. Taheri, E. "Any-time randomized kinodynamic path planning algorithm in dynamic environments with application to quadrotor." ***International Journal of Engineering, Transactions A: Basics***, Vol. 34, No. 10, (2021), 2360-2370. doi: 10.5829/ije.2021.34.10a.17

28. Kumar, P., and Chaudhary, S., K. "Stability and robust performance analysis of fractional order controller over conventional controller design." ***International Journal of Engineering, Transactions B: Applications***, Vol. 31, No.2, (2018), 322-330. doi: 10.5829/ije.2018.31.02b.17

Persian Abstract

چکیده

در این مقاله، یک روش ادراک بیونیک موقعیت کندن پرتقال ناف بر اساس Fmincon و کنترل زاویه متناسب -دیفرانسیل (PD) برای حل مشکلات آشفتگی باد و شاخه‌های سبز در محیط بدون ساختار پویا پیشنهاد شده است که باعث ایجاد اختلال بزرگ در فضای فضایی می‌شود .درک و کنترل پرتقال ناف در مرحله اول، یک مدل راه حل بهینه از زاویه چرخش هدف جهانی سیستم کنترل مبتنی بر Fminconبرای حل مشکل بهینه سازی زاویه حرکت رویکرد هدف ربات ایجاد شده است .ثانیا، یک سیستم ادراک بیونیک از موقعیت چیدن بر اساس کنترل زاویه PD برای حل مشکلات ادراک خاص ساخته شده است .در نهایت، یک پلت فرم شبیه‌سازی مشترک برای انتخاب ربات‌ها بر اساس Solidworks، Adamsو Simulinkتوسعه داده می‌شود و اعتبار و دقت الگوریتم تأیید می‌شود .نتایج تجربی نشان می‌دهد که میزان دقت برداشت 95درصد است، خطای زاویه هر مکانیزم بیش از 0.5درجه نیست، خطای جابجایی کمتر از 10میلی‌متر است و کل زمان از محاسبه زاویه بهینه تا پایداری سیستم فقط در حدود است 0.33 .ثانیه این روش برای درک سریع موقعیت چیدن و کنترل زاویه فعال ربات‌های چیدن در محیط بدون ساختار پویا مناسب است.